

A study on fracture energy of notched plain blended cement concrete beams with notch at varying positions

Varsha Gokak^{1,2*} , K.G. Vishwanath^{1,2}

¹ Department of Civil Engineering, Jain College of Engineering, Ts Nagar, Hunchannati Cross, Machche, India

² Affiliated To Visveswaraya Technological University, Belagavi, Karnataka, India

* Corresponding author's e-mail: varsha.gokak87@gmail.com

ABSTRACT

Fracture mechanics is the bridge in understanding the failure behaviour of plain concrete beams are subjected to different loading conditions. Fly ash and ground granulated blast furnace slag (GGBS) are widely used supplementary cementitious materials (SCMs) that enhance concrete performance while reducing environmental impact. Hence, the present study investigated the fracture energy of notched plain blended concrete beams with fly ash and GGBS with varying lengths, a/d ratios and varying notch positions. A series of experimental tests, from fresh concrete tests to hardened concrete tests including three-point bending are conducted to evaluate the fracture energy on 3 different sized beams with varying depth as well as notch depth and notch position. The results highlight the influence of geometric variations on fracture behaviour. It is seen that length of the beam, depth of the beam along with the varying notch depth and position of notch contribute to the variation of fracture energy.

Keywords: fracture energy, a/d ratio, fly ash and GGBS concrete, three-point bending, notched beam, fracture mechanics.

INTRODUCTION

Plain blended cement concrete

Using fly ash and ground granulated blast furnace slag (GGBS) as supplementary cementitious materials (SCMs) in concrete has been extensively researched. They have positive effects on the environment and performance, including lower carbon emissions, increased durability, and easier workability. The main constituents of fly ash, a by-product of burning coal, are iron oxides, silica, and alumina. It increases the workability and durability of concrete. Rich in calcium silicates, GGBS is a by-product of iron manufacturing that improves the resilience to sulphates and durability of concrete, as well as practicality, because of its spherical particle shape, Smith et al. [1] showed that addition of fly ash improves the workability of fresh concrete. According to Patel and Kumar [2], mixing GGBS enhances flowability and lessens the use for superplasticizers or water. The

long-term strength of concrete is enhanced by fly ash. After 28 days, concrete with 30% fly ash replacement has a compressive strength that is equal to regular Portland cement (OPC) concrete, according to Jones and Lee [3]. Conversely, GGBS speeds up the development of strength in the early years. A combination of fly ash and GGBS up to 50% offers a balanced strength growth profile, according to the research by Roy et al. [4]. Considering durability, blended concrete has exceptional durability properties. Fly ash and GGBS increase resistance to sulphate attack and chloride ion penetration, according to the research by Gupta et al. [5]. Furthermore, concrete compositions with 40% GGBS and 20% fly ash showed improved freeze-thaw resistance, according to Yang and Zhao [6]. The advantages for the environment are that concrete manufacturing has a lower carbon footprint when fly ash and GGBS are used. Every ton of fly ash used in concrete lowers CO₂ emissions by about 0.9 tons, according to Thomas [7]. Similar

advantages are provided by GGBS, which lowers waste disposal and energy use Singh & Verma [8].

Fracture parameters

Fracture energy, fracture stiffness, and ductility factor etc. are the fracture parameters which play a crucial role in determining the mechanical behaviour of plain concrete beams. According to Bažant and Planas [9], fracture energy is influenced by specimen size, aggregate distribution, and notch depth, all of which significantly impact crack initiation and propagation. Experimental studies by Carpinteri et al. [10] showed that increasing beam depth leads to higher fracture energy values due to an extended fracture process zone. Furthermore, research by Rilem [11] presented standard methods for determining the fracture energy, providing a base line for comparative study of results from different experimental setups.

Fracture energy in plain concrete

Fracture energy in plain concrete indicates how well the material can withstand the spread of cracks. By changing the microstructure, decreasing porosity, and boosting crack resistance, Lee and Wong [12] concluded that the addition of fly ash and GGBS enhances fracture energy. Additionally, Silva, Das, and Chatterjee [13] found that using SCMs in place of up to 40% of regular portland cement can result in a 15% increase in fracture energy, indicating the potential of blended materials to improve the toughness of plain concrete.

Significance of fracture energy

Concrete is a quasi-brittle material with complex fracture behaviour that cannot be fully described by conventional strength-based theories. Fracture mechanics provides a more accurate assessment of crack initiation, propagation, and ultimate failure in concrete structures. In the present study, analysing fracture energy in notched plain blended cement concrete beams of varying lengths, varying a/d ratios (“ a ” is the depth of notch and “ d ” is the depth of beam) and notches placed at two dissimilar positions was carried out.

Analytical and numerical methods have also been employed to study fracture mechanics in concrete beams with change in dimensions. Jirásek and Bažant [14] utilised finite element analysis (FEA) and extended finite element method (XFEM) to simulate crack growth and

stress dispersal in notched beams. Their findings demonstrated that fracture stiffness decreases with increasing notch depth, reducing the overall load-bearing capacity of the beam. Shah et al. [15] highlighted the significance of ductility factor in assessing energy dissipation capacity, noting that deeper beams exhibit improved post-peak deformation behaviour. These studies emphasise the necessity of integrating experimental and computational methods to achieve a comprehensive understanding of fracture mechanics in plain concrete beams. Predicting crack propagation and failure modes in concrete structures requires an understanding of fracture energy. While plain concrete depends on optimum mix designs to obtain increased toughness, reinforced concrete (RC) exhibits greater post-cracking performance due to reinforcement, yet both types of concrete benefit from improved fracture energy [16].

Relationship between fracture energy (G_f) and stress intensity factor (K) for plain concrete beams

Fracture energy (G_f) and the stress intensity factor (K) are critical parameters for analysing the cracking behaviour of concrete, as demonstrated by Xu, Zhang [17]. The interplay between these properties delivers insight the toughness and crack propagation resistance of plain concrete beams. In plain concrete, the relationship between G_f and K is more directly dependent on the intrinsic properties of the concrete matrix. Wang and Huang [18] demonstrated that fracture energy correlates strongly with the aggregate size and binder composition, with larger aggregates and the incorporation of SCMs such as fly ash and GGBS enhancing toughness. Silva et al. [13] found that higher fracture energy values correspond to greater resistance to crack initiation, reflected in an elevated critical stress intensity factor.

Fracture energy of notched beams

One of the first and most significant investigations into fracture energy in notched concrete beams was carried out by Bazant and Oh [19]. By comparing their results with experimental data, they showed that fracture energy is size-dependent and impacted by aggregate interlocking mechanisms. Prior experimental research on fracture energy under static, quasi-static, and dynamic stress conditions was examined by Ulfkjaer et al.

[20], their results showed that because of the rate-dependent behaviour of concrete, higher loading rates result in larger fracture energy. Mobasher, Khayat et al. [21] examined how loading rate and notch-to-depth ratio interact to affect the flexural performance of ultra-high-performance concrete (UHPC).

A notch can be positioned at various points to examine the impact of crack initiation and propagation when examining the fracture energy of a notched beam. The following are the most typical notch positions:

1. Standard position i.e. Central Notch (Mid-Span) – this is standard case in fracture mechanics which investigations and results in stable crack growth. It simulates a fracture in Mode I (pure opening).
2. Asymmetrical Off-Centre Notch – in this case, the fracture behaviour under mixed-mode loading (Mode I + Mode II) is investigated. It aids in researching crack deviation and shear effects according to Shah, Swartz, Ouyang, [15]. The calculation does not take into consideration shear stresses (Mode II), which are introduced by a notch at a different place given by Bazant & Planas, [9] but Tada et al. [22] suggest that off-centre notches change force equilibrium, potentially affecting energy calculations.

Empirical correlations

Meng et al. [23] carried out computation of flexural tensile strength in notched beams by examining the effects of loading rate and notch-to-depth ratio on the flexural performance of ultra-high-performance concrete beams. They used the three-point bending test to assess the flexural strength of notched UHPC beams. The flexural strength is determined using the following formula:

$$f_u = \frac{3P_u L}{2b(d-a_0)^2} \quad (1)$$

where: f_u – ultimate flexural strength, P_u – ultimate Load, L – effective length, b – width of the beam, d – depth of the beam, a_0 – depth of notch.

According to Rilem [11] and Hillerborg [24], fracture energy is the average energy determined by dividing the work of fracture by the projected fracture area. It is also described as the area under the load-CMOD curve per unit of fractured surface.

$$G_f = \frac{(W_f)}{(d-a_0)t} \quad (2)$$

where: W_f – area below the load displacement curve, d – depth of beam, a_0 – initial crack length/depth of notch, t – thickness of beam.

To account for mixed-mode fracture effects (combining Mode I, or tensile opening, and Mode II, or shear), Rilem [11] suggested correction factors that must be given to concrete beams with a notch at different places. The following formula can be used to calculate the adjusted fracture energy.

$$G_f = \frac{(\eta)W_f}{(d-a_0)t} \quad (3)$$

where: G_f – corrected fracture energy, W_f – total work of fracture, D – beam depth, a_0 – initial notch depth, t – beam thickness, η – correction factor accounting for the notch position.

The placement of the notch and the loading configuration, such as three-point or four-point bending, determine the correction factor η . Empirical values for various notch positions have been suggested by research studies. Shear effects affect fracture energy in three-point bending beams with an off-centre notch at $L/3$, rather than the centre. An approximation of correction factor accounting for the notch position is given by

$$\eta = 1 + \alpha \left(\frac{x}{L} \right) \quad (4)$$

where: α – empirical factor (ranges from 0.2 to 0.5 based on experimental studies), x – notch location from the nearest support (m), L = beam span (m).

METHODOLOGY

Materials and mix design

The flexural performance and fracture behaviour of plain mixed concrete beams under static loading were experimentally investigated. Various-sized beam specimens were cast in accordance with the mix proportion. In the study, 20 mm downsize coarse aggregate was utilized. A sawing machine was used to create various notches in beam specimens; 0.25, 0.33, and 0.5 were the notch to depth ratios taken into consideration. Every beam size and notch depth ratio had three identically cast specimens. After 24 hours

of casting, all specimens were demoulded, and they were allowed to cure for 28 days. The water-to-cement ratio of the normal concrete mix was 0.5. The cement in the current investigation was replaced with blended concrete that contains 20% fly ash and 10% GGBS. Bureau of Indian Standards, IS 10262: Concrete mix proportioning – Guidelines [25] was used to design the M25 concrete mix. The type of cement used in this study was ordinary portland cement (OPC) 43 grade as per Bureau of Indian Standards IS 8112-1989 [26]

Specification for 43 Grade ordinary portland cement. Conplast SP430, A high-range water reducer based on sulfonated naphthalene formaldehyde (SNF) super plasticizer is employed throughout the experimental work in the current investigation to improve workability and slump. The concrete mix slump was 80 mm, and its 28-day compressive strength was 32.86 N/mm² for the M25 grade design mix.

Specimen preparation

The blended concrete plain beams were cast in different lengths, such as 700 mm, 1200 mm, and 1500 mm along with constant width (b) of 150 mm and varying depths (d) of 150 mm, 250 mm, and 350 mm (Fig. 1, 1). A regulated notch of depth “a” was incorporated into each beam to

aid in fracture investigation. For plain concrete blended beams, the notch depth was set based on a/d ratio, (where “a” is the depth of notch) of 0.25, 0.33, and 0.5. The study includes 2 different positions of the notches, viz. one at the centre of beam and second position was at the 1/3rd length of beam (1/3). The data was elaborated in Table 1.

To evaluate the Fracture Energy, the deflection properties need to be recorded by performing a three-point bending test. Standardized tests, such the three-point bending test on notched beams, are frequently used to evaluate fracture energy. A displacement-controlled flexural testing equipment and a real-time data collecting machine make up the experimental setup. A strain-controlled test is one in which the strain is increased at a constant, uniform pace and the test is carried out in that manner.

The tests were carried out on the specimens under crack mouth opening displacement control at a consistent pace of 0.02 mm/min. To measure crack mouth opening displacement (CMOD), a clip gauge was used. The downward displacement was measured using a linear variable displacement transducer (LVDT). To measure the downward displacement at mid-span, a LVDT was employed and also some manual readings were noted down. The area under the load-deflection curves up to the failure point was used to calculate the

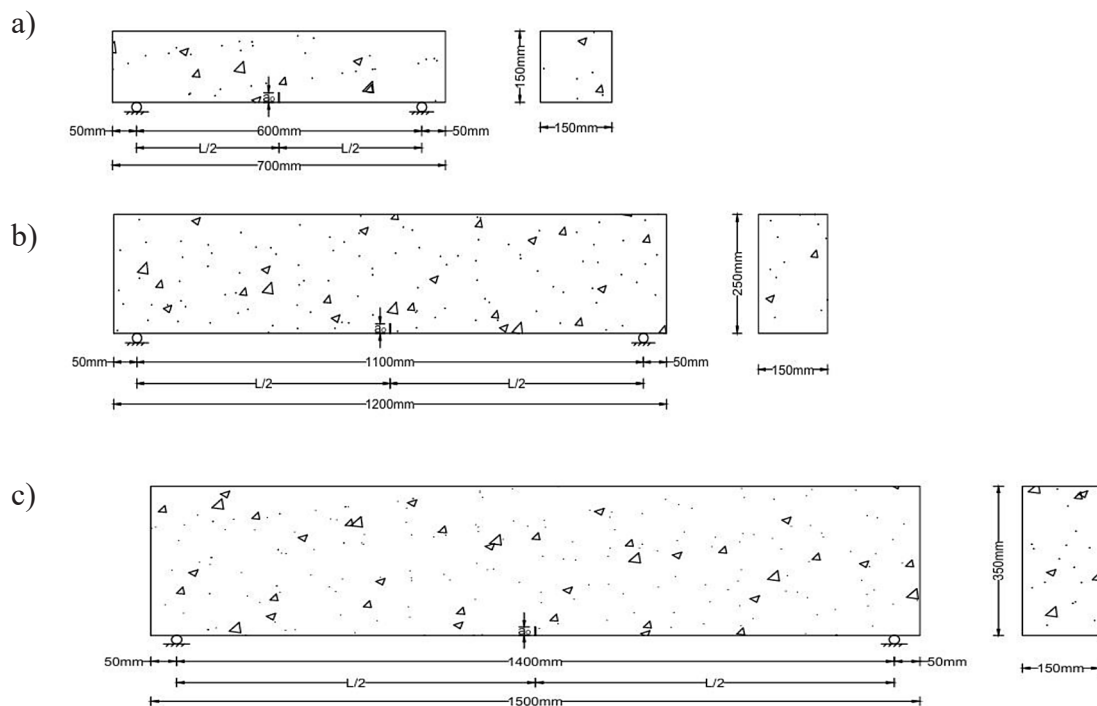


Figure 1. Plain beam of length (a) 700 mm, (b) 1200 mm, and (c) 1500 mm with notch at centre (L/2) and their cross-section dimensions

Table 1. Table showing the details of the specimens and parameters considered

Sl.No	Position of notch	Notch to depth ratio a/d or a_v/d	Length (L) mm	Effective length (l) mm	Breadth(b) mm	Depth (d) mm	Depth of notch (a_0) mm
1.	Notch At Centre $l/2$	0.25	700	600	150	150	37.5
2.		0.33	700	600	150	150	49.5
3.		0.5	700	600	150	150	75
4.		0.25	1200	1100	150	250	62.5
5.		0.33	1200	1100	150	250	82.5
6.		0.5	1200	1100	150	250	125
7.		0.25	1500	1400	150	350	87.5
8.		0.33	1500	1400	150	350	115.5
9.		0.5	1500	1400	150	350	175
10.	Notch at $1/3^{rd}$ Length $l/3$	0.25	700	600	150	150	37.5
11.		0.33	700	600	150	150	49.5
12.		0.5	700	600	150	150	75
13.		0.25	1200	1100	150	250	62.5
14.		0.33	1200	1100	150	250	82.5
15.		0.5	1200	1100	150	250	125
16.		0.25	1500	1400	150	350	87.5
17.		0.33	1500	1400	150	350	115.5
18.		0.5	1500	1400	150	350	175

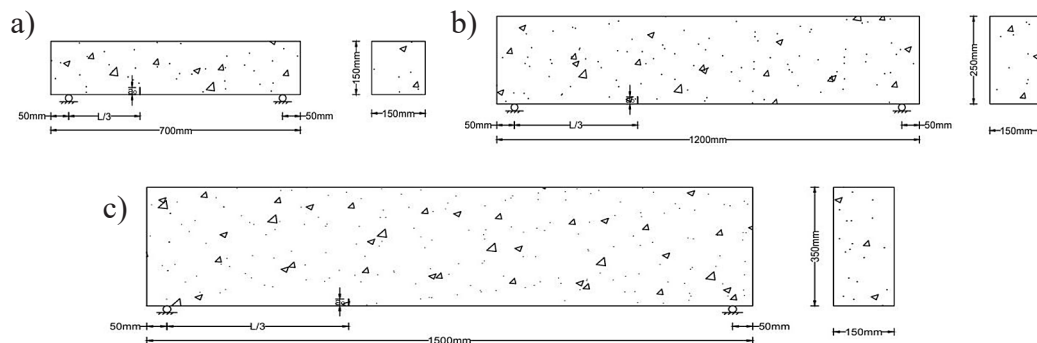


Figure 2. Plain beam of length (a) 700 mm, (b) 1200 mm, and (c) 1500 mm with notch at $L/3$ and their cross-section dimensions

energy. A notched concrete specimen had to be prepared as part of the procedure. By placing a load on at a steady pace, until the specimen fails, the load and deflection are recorded. Determining the fracture energy, which is the effort required to spread the crack and is frequently standardised by the cross-sectional area of the crack surface. The following results were obtained.

RESULTS AND DISCUSSION

The load deflection curves were plotted for all the 3 lengths of beams with notch to depth (a/d)

ratio of 0.25, 0.33 and 0.5, as shown in Figures 4, 5, and Table 2, 3.

From the Figures 3a, 3b and 4a, it is observed that the load carrying capacity of a larger beam ($L = 1500$ mm) is more compared to small beams ($L = 700$ mm) due to higher moment of inertia. Longer beams distribute the applied load over a greater span, reducing stress concentration at specific points compared to shorter beams and a larger beam typically has a higher section modulus, meaning it can withstand greater bending moments before failure. Also, if the larger beam has a greater depth, it will be stiffer and resist deflections better than a smaller beam with the same material properties.

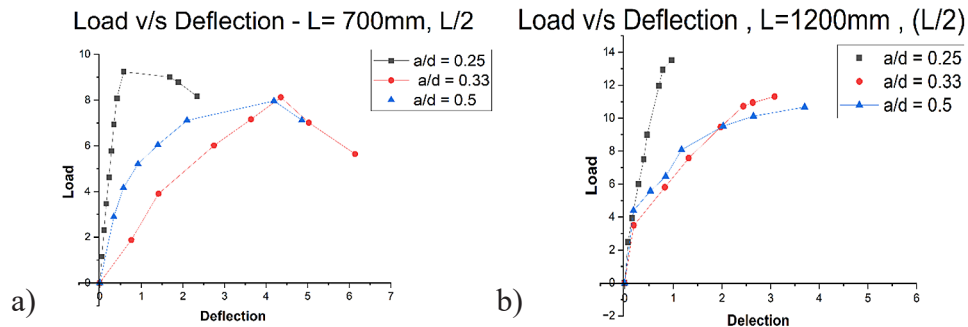


Figure 3. The load deflection curves for beams of lengths (a) 700 mm and (b) 1200 mm with the notch at the centre i.e. $L/2$ for various a/d ratios viz. 0.25, 0.33 and 0.5

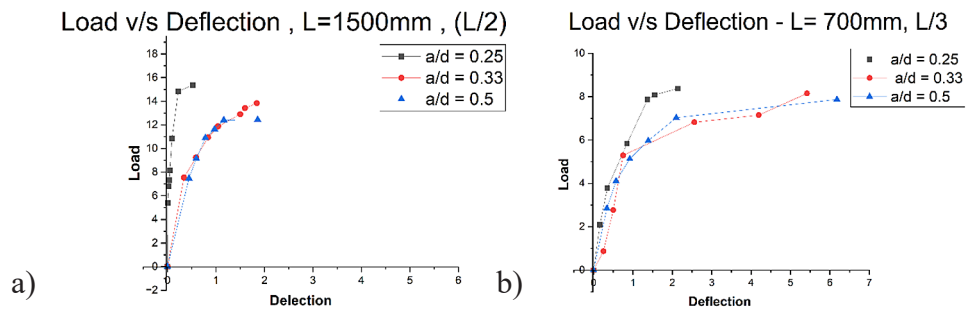


Figure 4. The load deflection curves for beams of lengths (a) 1500 mm when the notch is at centre along with the beam of length (b) 700 mm with the notch at $1/3^{\text{rd}}$ of length i.e. $L/3$ for various a/d ratios viz. 0.25, 0.33 and 0.5

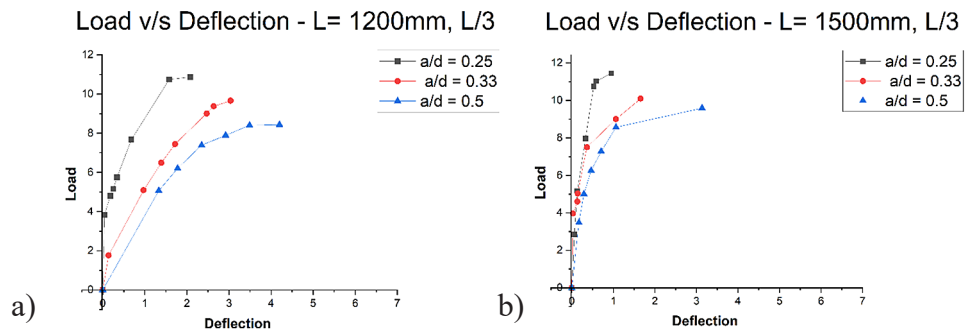


Figure 5. The load deflection curves for beams of lengths (a) 1200 mm and (b) 1500 mm when the notch is at $1/3^{\text{rd}}$ of length i.e. $L/3$ for various a/d ratios viz. 0.25, 0.33 and 0.5

Table 2. Fracture energy for plain blended concrete beams with notch at centre – $L/2$

Beam length L (mm)	Effective length l (mm)	Depth of beam d (mm)	a/d ratio	Depth of Notch a0 (mm)	Flexural tensile strength (MPa)	Fracture energy N/m
700	600	150	0.25	37.5	4.39	144.42
		150	0.33	49.5	4.84	214.17
		150	0.5	75	8.49	332.69
1200	1100	250	0.25	62.5	4.23	32.6
		250	0.33	82.5	4.43	97.98
		250	0.5	125	7.50	253.54
1500	1400	350	0.25	87.5	3.12	13.21
		350	0.33	115.5	3.52	53.94
		350	0.5	175	5.68	68.57

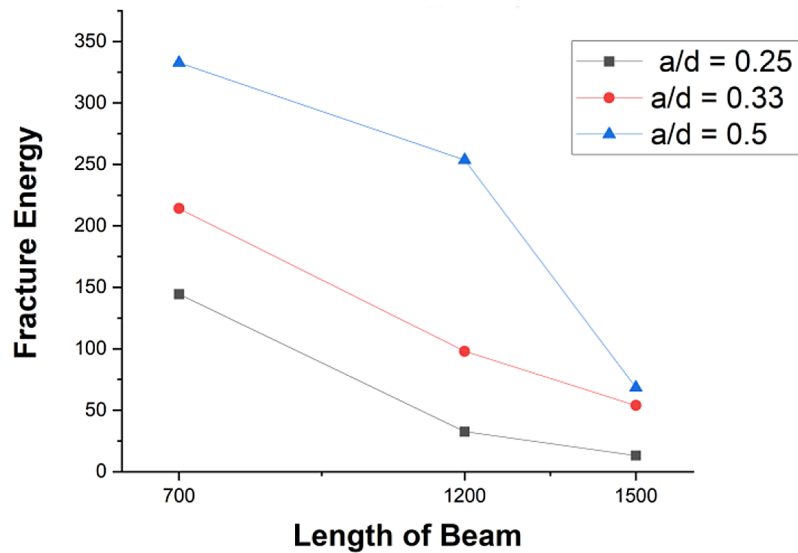


Figure 6. Fracture energy of beams with lengths 700 mm, 1200 mm, and 1500 mm along with the a/d ratio of 0.25, 0.33 and 0.5 with notch at the centre of beam

Table 3. Fracture energy for plain blended concrete beams with notch at 1/3rd distance (L/3)

Beam length (mm)	Effective length l (mm)	Depth of beam d (mm)	a/d ratio	Depth of notch a0 (mm)	Flexural tensile strength (MPa)	Corrected fracture energy N/m
700	600	150	0.25	37.5	3.97	85.64
		150	0.33	49.5	4.84	244.73
		150	0.5	75	8.39	394.64
1200	1100	250	0.25	62.5	3.40	72.03
		250	0.33	82.5	3.79	88.05
		250	0.5	125	5.93	200.03
1500	1500	350	0.25	87.5	2.49	23.61
		350	0.33	115.5	2.76	47.2
		350	0.5	175	4.70	111.18

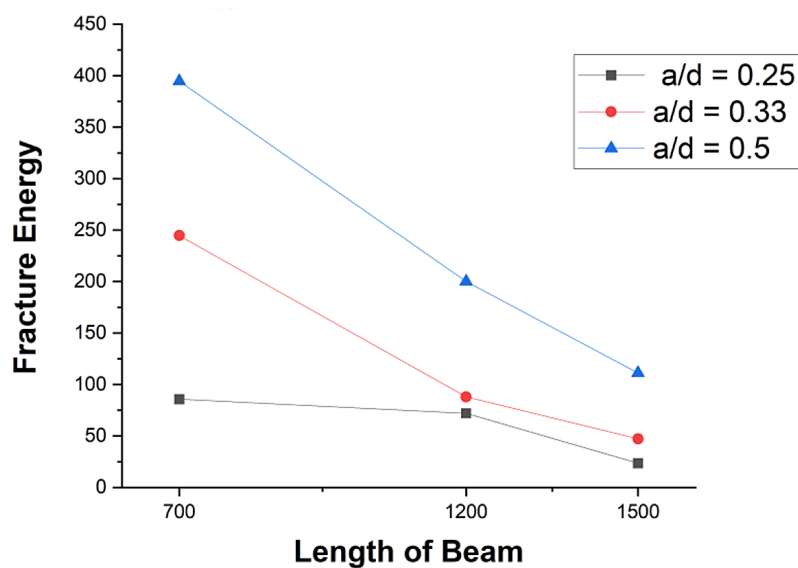


Figure 7. Fracture energy of beams with lengths 700 mm, 1200 mm and 1500 mm along with the a/d ratio of 0.25, 0.33, and 0.5 when notch is at 1/3rd of length i.e. (L/3) of beam

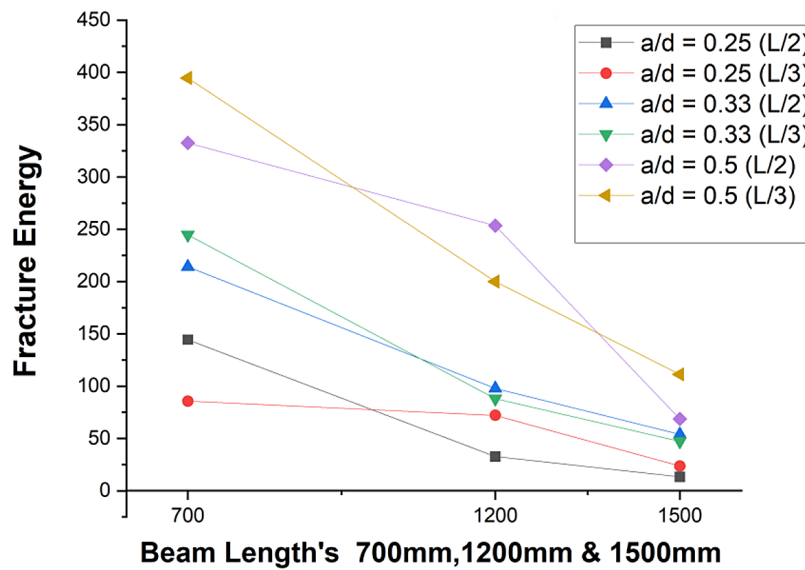


Figure 8. Comparative fracture energy of various beams with the a/d ratio of 0.25, 0.33, and 0.5 with notch at centre (L/2) and notch at 1/3rd of length i.e. (L/3)

A deeper notch affects a smaller beam more significantly, because it removes a larger percentage of the total cross-section, whereas in a larger beam, the same notch depth might have a lesser impact. In smaller beams, shear forces dominate, leading to earlier failure, while in larger beams, bending strength plays a greater role, allowing them to carry higher loads.

When the graphs with study of notch at centre i.e. 1/2 (Fig. 6 and Fig. 8) are compared with graphs with notch at 1/3 (Fig. 7 and Fig. 8), the load-carrying capacity of concrete notched beams with a notch at the centre is higher than beams with a notch at L/3 due to factors like the maximum bending moment occurs at the centre (L/2), while at L/3, the moment is slightly lower. A notch at L/3 is in a high shear zone, significantly reducing the beam shear capacity and making it more prone to sudden shear failure. Shear cracks caused by notches at L/3 can result in brittle failure quickly. Flexural cracks, which are primarily caused by central notches, form gradually and improve load dispersion prior to failure.

From Figure 8, it is seen that, for all three a/d ratios of 0.25, 0.33, and 0.5, the fracture energy for the length of 700 mm beam is the highest when compared to the 1200 mm and 1500 mm length beams, in both cases of notch at centre and notch at 1/3rd of length, because smaller beams (700 mm) have a smaller fracture process zone (FPZ), localised crack propagation occurs with a stronger resistance to total failure, resulting in higher fracture energy. As larger beams (1200 mm and

1500 mm) have a greater FPZ, cracking occurs more widely and requires less energy to propagate. Larger beams have more distributed cracking, which means the energy needed to propagate a crack is dispersed, resulting in a lower overall fracture energy. In shorter beams, the stress distribution around the notch leads to a higher energy absorption capacity before full fracture.

While fractures spread more readily in longer beams because of increased bending moments and less local toughness, the 700 mm beam offers higher energy absorption for all three a/d ratios, because the crack route is more concentrated. The notch at L/3 is a shear dominated failure and the notch at centre is a flexural failure.

Figure 8 shows that, for all beams with lengths of 700 mm, 1200 mm, and 1500 mm, the fracture energy is highest for an a/d ratio of 0.5 when compared to a/d ratios of 0.25 and 0.33. This might be due to Transition from Shear-Dominated to Flexural-Dominated Failure. Higher a/d ratio (0.5) shifts the failure mode towards flexural failure, which involves gradual crack propagation and requires more energy for full fracture. Shear stresses predominate for low a/d ratios (0.25, 0.33), resulting in a more abrupt and brittle collapse. Greater energy absorption by plastic deformation before to failure is made possible by the bending moment, which predominates at larger a/d ratios (0.5).

Abrupt deflection changes as seen in load deflection curves presented in Figures 3a, 3b, 4a.4b & 5a, 5b, which result from the quick beginning and spread of cracks in notched beams. In

contrast to automatic systems that record at pre-determined intervals, the data was manually recorded at times, which may have led to irregular gaps between points due to human judgment and response time. While more points were recorded during critical events such as crack formation or abrupt increases in deflection, fewer points were recorded in stable zones. Stress concentration at the notch causes brittle failure and decreased ductility in notched plain blended concrete beams, resulting in a single dominating crack. The beam suddenly loses its ability to support weight once the crack reaches a critical point, which frequently results in the testing apparatus losing load control. The data acquisition system (DAQ) may perceive this as test completion since it causes a dramatic force drop. The brittle nature of failure is thus confirmed by the load-deflection plots, which only record data up to the ultimate load of the beam without a progressive force decline.

Failure modes, stress concentration, and fracture mechanics are the main factors influencing the observed behaviour, as shown above. When the crack reaches a critical length, the notch tip works as a stress concentrator, causing a brittle collapse. Regardless of beginning stiffness, fracture is the predominant failure mode for $a/d = 0.33$ and 0.5 since there is very little ligament left. Increasing the notch to depth ratio past $a/d = 0.33$ has no discernible effect on the peak force since the fracture characteristics of blended concrete stay constant. Furthermore, GGBS and fly ash improve the microstructure of concrete, but not its post-cracking ductility, which causes it to fracture suddenly. A greater residual ligament, however, permits some redistribution of stress at $a/d = 0.25$, resulting in a higher peak force and behaviour more akin to flexural failure than fracture-dominated failure.

CONCLUSIONS

This study offers valued perceptions into the fracture mechanics of plain concrete blended beams with varying lengths and depths. The findings highlighted the importance of considering geometric variations in structural design and fracture analysis. They are in line with the literature that has been studied. Some of the conclusions drawn are:

1. Fracture energy exhibits significant dependency on specimen geometry.
2. The shorter beams will have higher fracture energy when compared to the longer beams

3. For beams with high notch depth (a), the fracture energy is less compared to the lower notch depth.
4. Fracture energy is maximum for $a/d = 0.5$ for all beam lengths, because the failure mode changes from shear to flexure, which causes cracks to propagate more energy-intensively. Flexural fissures gradually grow and absorb more force before breaking completely. Higher a/d ratios enable more energy dissipation through stress redistribution. Crack resistance is increased by the wider fracture process zone.
5. Shear-dominated failure when notch is at $L/3$ and flexural-dominated failure when notch at centre, both contribute to higher energy absorption in shorter beams.
6. Although it may lessen early-age strength, the addition of 20% fly ash and 10% GGBS typically improves long-term performance.
7. Flexural strength rises as span length increases, because a larger moment is applied to the beam. Flexural strength increases in line with notch depth as the effective depth decreases and stress concentration at the notch increases.

REFERENCES

1. Smith, J., Brown, C., & Adams, T. (2015). The impact of fly ash on fresh concrete properties. *Concrete Research Journal*, 18(3), 78–85.
2. Patel, R., & Kumar, S. (2017). Workability enhancement through GGBS in concrete mixtures. *Materials and Structures*, 50(7), 345–353.
3. Jones, M., & Lee, S. (2016). Long-term strength development in fly ash concrete. *International Journal of Civil Engineering*, 19(6), 412–420.
4. Roy, T., Bhandari, A., & Sen, P. (2018). Strength properties of fly ash and GGBS blended concrete. *Advanced Concrete Studies*, 15(2), 98–110.
5. Gupta, R., Singh, K., & Malik, A. (2019). Durability characteristics of blended concrete. *Journal of Concrete Research*, 21(4), 233–245.
6. Yang, X., & Zhao, L. (2020). Freeze-thaw resistance in fly ash and GGBS blended concrete. *Cold Climate Concrete Research*, 7(5), 321–330.
7. Thomas, M. (2019). Environmental impact of SCMs in concrete. *Green Concrete Advances*, 8(4), 200–215.
8. Singh, M., & Verma, R. (2021). Sustainability in concrete using GGBS: A review. *Environmental Materials Review*, 10(1), 56–64.
9. Bažant, Z. P., & Planas, J. (1998). *Fracture and size effect in concrete and other quasi-brittle materials*. CRC Press.

10. Carpinteri, A., Bocca, P., & Valente, S. (2010). Experimental analysis of fracture mechanisms in concrete. *Engineering Fracture Mechanics*, 77(6), 987–1003.
11. RILEM. (2004). Recommendation for determining fracture energy of concrete. *Materials and Structures*, 37(10), 569–576.
12. Lee, J., & Wong, K. (2018). Fracture properties of plain concrete with fly ash and GGBS. *Concrete Research Letters*, 9(3), 245–253.
13. Silva, M., Das, A., & Chatterjee, S. (2018). Fracture properties of plain concrete with SCMs. *Materials Research Journal*, 25(2), 115–127.
14. Jirásek, M., & Bažant, Z. P. (2002). *Inelastic analysis of structures*. John Wiley & Sons, *Materials and Structures*, 16(93), 155–177. <https://doi.org/10.1007/BF02472495>
15. Shah, S. P., Swartz, S. E., & Ouyang, C. (1995). *Fracture mechanics of concrete: Applications of fracture mechanics to concrete, rock, and other quasi-brittle materials*. John Wiley & Sons.
16. Zhao, L., & Li, X. (2021). Fracture mechanics in reinforced concrete: An overview. *Structural Engineering Advances*, 18(2), 110–120.
17. Xu, Q., & Zhang, Y. (2022). Empirical modelling of G_f and K relationships in concrete. *Journal of Civil Engineering Materials*, 21(4), 355–368.
18. Wang, Z., & Huang, R. (2020). Aggregate influence on fracture energy in concrete beams. *Journal of Building Materials Research*, 14(6), 245–259.
19. Bažant, Z. P., & Oh, B. H. (1983). Crack band theory for fracture of concrete. *Materials and Structures*, 16(3), 155–177. <https://doi.org/10.1007/BF02486267>
20. Ulfkjær, J. P., Hansen, L. P., Qvist, S., & Madsen, S. H. (1996). Fracture energy of plain concrete beams at different rates of loading. *WIT Transactions on The Built Environment*, 25, 11–20. <https://doi.org/10.2495/SUSI960381>
21. Meng, W., Yao, Y., Mobasher, B., & Khayat, K. H. (2017). Effects of loading rate and notch-to-depth ratio of notched beams on flexural performance of ultra-high-performance concrete. *Cement and Concrete Composites*, 83, 349–359. <https://doi.org/10.1016/j.cemconcomp.2017.07.026>
22. Tada, H., Paris, P. C., & Irwin, G. R. (2000). *The stress analysis of cracks handbook* (3rd ed.). ASME Press.
23. Meng, W., Yao, Y., Mobasher, B., & Khayat, K. H. (2017). Effects of loading rate and notch-to-depth ratio of notched beams on flexural performance of ultra-high-performance concrete. *Cement and Concrete Composites*, 84, 162–173. <https://doi.org/10.1016/j.cemconcomp.2017.07.026>
24. Hillerborg, A., Modéer, M., & Petersson, P. E. (1976). Analysis of crack formation and crack growth in concrete by means of fracture mechanics and finite elements. *Cement and Concrete Research*, 6*(6), 773–782.
25. Bureau of Indian Standards. (2019). IS 10262: Concrete mix proportioning – Guidelines. Bureau of Indian Standards.
26. IS 8112:1989 – Specification for 43 grade ordinary Portland cement. Bureau of Indian Standards.